

Swelling and Contraction of the Mitochondrial Matrix

II. QUANTITATIVE APPLICATION OF THE LIGHT SCATTERING TECHNIQUE TO SOLUTE TRANSPORT ACROSS THE INNER MEMBRANE*

(Received for publication, April 3, 1985)

Keith D. Garlid and Andrew D. Beavis

From the Department of Pharmacology, Medical College of Ohio, Toledo, Ohio 43699

The relationship between matrix volume and the amount of light scattered by a mitochondrial suspension has been characterized for equilibrium measurements and shown to depend in a complex but predictable manner on native structure of the mitochondrion (Beavis, A. D., Brannan, R. D., and Garlid, K. D. (1985) *J. Biol. Chem.* 260, 13424-13433). In the present report, we show that this characterization also applies to kinetic measurements of salt and nonelectrolyte transport. We derive and evaluate quantitative methods for determining permeability constants from light scattering kinetics. We apply these equations to the problem of whether matrix swelling itself induces permeability changes secondary to membrane stretching or changes in surface available for transport. A study of erythritol transport over a 7-fold range of matrix volume reveals dramatic changes in light scattering rates, as previously observed (Tedeschi, H. (1959) *J. Biophys. Biochem. Cytol.* 6, 241-252). These transitions correspond exactly to structure-dependent transitions in the relationship between absorbance and matrix volume. When this is taken into account, erythritol permeability is found to be constant over the entire volume range. Factors affecting intrinsic membrane porters, such as Mg^{2+} depletion and dicyclohexylcarbodiimide, are also found to be without effect on erythritol permeability. The broader significance of this study is that the light scattering technique is shown to be capable of providing quantitative answers to important questions about solute transport across the inner membrane.

Net transport of solutes across the inner membrane of mitochondria is accompanied by transport of water, resulting in swelling or contraction of the matrix compartment. Water permeation, in turn, is sufficiently rapid to assure that osmotic equilibrium is maintained and that the rate of swelling is limited by the rate of solute transport (1, 2). Thus, a technique for quantitative measurement of matrix swelling rates would be a powerful tool for the study of transport mechanisms in mitochondria. The light scattering (LS^1) technique, in which matrix swelling causes a decrease in the intensity of light scattered by the suspension (3, 4), would seem to be ideally suited to this purpose.

Efforts by Tedeschi and co-workers (2, 5, 6) to develop quantitative LS methodology were met by strong reservations

* This research was supported in part by United States Public Health Service Grant GM 31086. The costs of publication of this article were defrayed in part by the payment of page charges. This article must therefore be hereby marked "advertisement" in accordance with 18 U.S.C. Section 1734 solely to indicate this fact.

¹ The abbreviations used are: LS, light scattering; mosm, milliosmolar; Φ , osmolality; TES, *N*-tris[hydroxymethyl]methyl-2-aminoethanesulfonic acid; DCCD, *N,N'*-dicyclohexylcarbodiimide.

and incomplete acceptance (7-10). Consequently, the LS technique is used today as it has been used for over 30 years (10-13), primarily as a qualitative assay of solute transport. A major reason for this state of affairs is that the existing quantitative models (2, 5, 6, 14, 15) failed to account for the complexity of the LS response. Thus, the dependence of A on mitochondrial concentration and the dependence of A^{-1} on matrix volume are both nonlinear (1). While Tedeschi *et al.* (5, 16) and Massari *et al.* (14) recognized these deviations, they did not provide methods for dealing with them. In the previous paper (1), we described the factors determining the equilibrium relationship between LS and matrix volume and showed how this relationship could be treated quantitatively. In the present report, we show how these findings may be applied to kinetic studies of solute transport across the inner membrane.

Transport of erythritol has been studied in detail. We show that DCCD and Mg^{2+} depletion, both of which profoundly affect ion porters in mitochondria (reviewed in Ref. 17), are without effect on erythritol transport. Previous workers have concluded from LS kinetics that matrix swelling causes accelerated solute transport. Azzone and co-workers (18-24) invoke "membrane stretching" to account for the apparent permeability increase. Tedeschi (6) concludes that the area accessible to polar solutes, such as erythritol, increases as the cristae unfold while the area accessible to more rapidly transported solutes, such as malonamide, is unaffected by swelling. The alternative explanation, that it is the equilibrium relationship between LS and matrix volume which changes (1) and that permeability and area remain constant, has not heretofore been considered. In this report, we show that the acceleration in LS kinetics has its origin in the nonlinear dependence of A^{-1} on matrix volume (1). When this is taken into account, we find no change in inner membrane permeability to erythritol over a 7-fold range of medium osmolalities. LS kinetic curves for malonamide uptake are superimposable on those for erythritol uptake when the time axes are properly scaled, showing that the LS measurement is well-behaved and that there is no qualitative difference in the transport of these two solutes. These applications illustrate the ability of the LS technique to resolve important qualitative and quantitative issues relating to inner membrane transport.

EXPERIMENTAL PROCEDURES²

RATIONALE

Relationship between Solute Transport Rates and Absorbance Measurements—Equation 1 permits normalization of

² Portions of this paper (including "Experimental Procedures" and Figs. 1-6, 8, and 12) are presented in miniprint at the end of this paper. Miniprint is easily read with the aid of a standard magnifying glass. Full size photocopies are available from the Journal of Biological Chemistry, 9650 Rockville Pike, Bethesda, MD 20814. Request Document No. 85M-1063, cite the authors, and include a check or money order for \$6.80 per set of photocopies. Full size photocopies are also included in the microfilm edition of the Journal that is available from Waverly Press.

absorbance measurements to the concentration, P , of mitochondrial protein in the assay medium:

$$\beta = \frac{P}{P_s} (A^{-1} - a) \quad (1)$$

where a is a machine constant equal to the y intercept of a plot of A^{-1} versus P^{-1} , and P_s (1 mg/ml) is a normalizing device to make β a dimensionless quantity (1). The expression relating β to the osmotically active matrix water content, W_i , of the mitochondrion was shown (1) to be:

$$\beta_j = \beta_j^0 + \frac{b_j W_i}{S_o} \quad (2)$$

where b_j (mosm) is the slope, β_j^0 is the intercept of the j th segment of the absorbance osmotic curve, and S_o (nosmol/mg) is the endogenous matrix solute content.

Equation 2 applies to changes in osmolality at constant matrix solute content. In principle, it should also apply to changes in solute content at constant osmolality. We limit consideration (a) to conditions under which endogenous solute content, S_o , remains constant during the phase of solute uptake and (b) to conditions under which water movement is sufficiently rapid with respect to solute uptake to assure osmotic equilibrium at all times. Accordingly, matrix water content can be written:

$$W_i(t) = \frac{S_o + nX_i(t)}{\Phi} \quad (3)$$

where X_i is the amount of matrix salt or nonelectrolyte transported into the matrix at time t , and n is the number of osmotically active solutes into which X dissociates. For present purposes, we are ignoring the contribution of the osmotic coefficient of the matrix solution. Differentiating Equation 2 with the aid of Equation 3, and introducing v (min^{-1}) for measured rate, we obtain the following.

$$v = \frac{d\beta}{dt} = \frac{nb_j}{\Phi S_o} \frac{dX_i}{dt} \quad (4)$$

Note that all LS rate measurements, v , depend on the value of the osmotic slope, b_j , which pertains to the matrix volumes over which the rate measurements are taken.

The Initial Rate Equation—We may write a general expression for uptake of solute into the matrix:

$$\frac{dX_i}{dt} = k([X]_o - [X]_i) \quad (5)$$

where $[X]_o$ and $[X]_i$ represent medium and matrix concentrations of X , respectively, and the transport rate constant, k , is the product of the permeability constant and the surface area of the inner membrane (6, 15). If rates are expressed in $\text{nmol}(\text{mg} \cdot \text{min})^{-1}$ and concentrations in millimolar, k has the dimensions $\mu\text{l}(\text{mg} \cdot \text{min})^{-1}$. Combining Equations 4 and 5 under initial conditions ($[X]_i = 0$),

$$v(\text{initial}) = \frac{nb_j}{\Phi S_o} k[X]_o \quad (6)$$

Equation 6 enables k to be obtained from initial rates of swelling in a medium consisting of a known concentration of permeant solute.

The Integrated Rate Equation— $[X]_o$ may be expressed as a simple function of medium osmolality:

$$[X]_o = \frac{c_w(1-f)}{n} \Phi \quad (7)$$

where f is the fraction of total osmolality contributed by

impermeant solutes, and $c_w(\text{g/ml})$ is the concentration of water in the solution. We make the approximation that c_w is the same on both sides of the membrane. Then, with the aid of Equations 3 and 7, Equation 5 may be written

$$\frac{dW_i}{dt} = c_w k \left\{ \frac{W_i^0}{W_i} - f \right\} \quad (8)$$

where $W_i^0 = S_o/\Phi$, the matrix water content prior to transport of X . Integration of Equation 8 yields

$$(W_i - fW_i^0)^2 = (1-f)^2(W_i^0)^2 + 2c_w W_i^0 k t \quad (9)$$

Using Equation 2 to express volumes in terms of β , S_o , and Φ , Equation 9 may be rearranged to give

$$\left(\beta - \beta_j^0 - \frac{fb_j}{\Phi} \right)^2 = (1-f)^2 \left\{ \left(\frac{b_j}{\Phi} \right)^2 + \frac{2b_j^2 c_w k t}{\Phi S_o} \right\} \quad (10)$$

If $f = 0$, Equation 9 reduces to the equation used by Tedeschi (6) and others (29), and Equation 10 becomes

$$(\beta - \beta_j^0)^2 = \left(\frac{b_j}{\Phi} \right)^2 + \frac{2b_j^2 c_w k t}{\Phi S_o} \quad (11)$$

Thus, a plot of $(\beta - \beta_j^0 - fb_j/\Phi)^2$ versus time should yield a slope proportional to k . Note that the value of β_j^0 used must be appropriate to the range of β values over which the slope is measured.

RESULTS

Quinine-induced Swelling in 275 mosm NH_4SCN —Quinine-induced swelling in NH_4SCN is dependent on the amount of quinine added (30), as illustrated in Fig. 1. All traces show an initial rapid rate of increase in β followed by a decline and then a second rapid increase. The transition point, estimated by solving linear equations fitted to each trace prior to and following the transition, is independent of time but occurs at the same value of β (0.172 ± 0.002) in each trace.

The transition point in the equilibrium osmotic curve also occurs at $\beta = 0.17$ (1), and the results in Fig. 1 constitute independent evidence for the conclusion of the previous paper that the transition from one linear region to another on the absorbance osmotic curve depends solely on matrix volume. Thus, uptake of solutes and water in 275 mosm medium ($\beta = 0.15$) follows one segment of the osmotic curve until W_i is approximately 1.65 mg/mg ($\beta = 0.17$). Then, due to irreversible changes in membrane packing, the relationship between β and W_i changes, and there is an increase in $d\beta/dt$.

Quinine-induced Swelling in NH_4SCN Media of Varying Osmolality—The data in Fig. 2 confirm that the breaks in the kinetic curves of Fig. 1 reflect a volume-dependent change in the LS properties of mitochondria. In this series, the dose of quinine was kept constant while the osmolality was varied from 55 to 275 mosm. The lower four traces of Fig. 2, obtained in NH_4SCN media ranging from 275 to 110 mosm, exhibit a break at the same point, 0.170 ± 0.003 ($n = 9$). As the starting β increases, the duration of the initial slow phase decreases. In media with lower osmolalities, the break is eliminated, supporting the conclusion that the break represents a volume-dependent change in LS properties.

We can construct an absorbance osmotic curve from these data using values of β determined 0.1 min prior to the addition of quinine. This curve (Fig. 3) shows a break, at about 0.16, close to the value of β at which the breaks occur in the kinetic traces of Figs. 1 and 2.

Matrix Swelling Due to Erythritol Transport—Erythritol is a small neutral solute whose transport is thought to occur independently of membrane porters. Fig. 4 contains a sample

of kinetic curves obtained in media of varying erythritol concentrations in which erythritol itself provides the main osmotic support. Note that a transition occurs at $\beta = 0.17$, after which the rate increases. Tedeschi (6) observed the same acceleration and, since he did not recognize the first break in the osmotic curve, attributed it to a real increase in solute and water transport. Our previous results (1) suggest, to the contrary, that the acceleration reflects an increase in non-matrix volume as the matrix swells. Swelling in erythritol provides a good model for evaluating these differing interpretations.

We have demonstrated that preswelling eliminates the sharp breaks which occur in the osmotic curve (1). We would predict, therefore, that a hypotonic pretreatment should also eliminate the breaks in the kinetic curves. Fig. 5 contains a series of traces obtained using preswollen mitochondria. The erythritol media were identical in composition to those used for Fig. 4. As predicted, the transition seen in the curves of Fig. 4 is eliminated by preswelling.

Construction of Osmotic Curves—Kinetic data similar to those contained in Figs. 4 and 5 were extrapolated to zero time, and the resulting β values were used to construct the osmotic curves plotted in Fig. 6. *Curve a* of Fig. 6, obtained from normal mitochondria, is similar to the equilibrium curve in tetraethylammonium Cl (1) and exhibits breaks at 116 and 70 mosm. *Curve b*, obtained with preswollen mitochondria, is essentially linear over the entire range, as previously observed. The slope of *curve b* is lower, reflecting loss of K^+ salts during preswelling and washing procedures.

For normal mitochondria, a break is observed at $\beta = 0.167$ in both the kinetic traces (Fig. 4) and the extrapolated osmotic curve (*curve a*, Fig. 6). For preswollen mitochondria, no break is observed in either the kinetic traces (Fig. 5) or the extrapolated osmotic curve (*curve b*, Fig. 6). This correlation suggests that the breaks in the kinetic and equilibrium curves have a common underlying cause and, therefore, cannot arise from a change in solute permeability or surface area.

Analysis of Initial Rate Measurements in Erythritol—Initial light scattering rates, v , were obtained from the records of Figs. 4 and 5 and adjusted for the observed osmotic slopes, b_j . Fig. 7 contains plots of these values for normal (*curve a*) and for preswollen (*curve b*) mitochondria. The data are plotted according to a rearranged version of Equation 6 which permits comparison of rates obtained from different segments of the osmotic curve:

$$\frac{\Phi}{b_j} v = \frac{k[X]_o}{S_o} \quad (12)$$

Since solute content, S_o , is constant for a given preparation, the curves should be linear with erythritol concentration, $[X]_o$, if k is constant over the entire range. This condition is fulfilled for both curves, indicating that the permeability to erythritol remains constant over the range of 42–280 mosm.

Nonlinearities in the LS response for normal mitochondria preclude obtaining accurate initial rates near the transition points, *i.e.* at erythritol concentrations between 150 and 270 mM. This disadvantage is overcome by using preswollen mitochondria (*curve b*, Fig. 7), which exhibit a linear osmotic curve over the range of study. We invariably observe, however, that the rate curve for preswollen mitochondria does not intercept zero, as predicted by Equation 12. This background rate of swelling may reflect lysis of fragile mitochondria, or it may reflect a time-dependence in the unfolding of membranes after transfer of mitochondria to the new medium. Whatever the explanation for the non-zero intercept, we consider it reasonable to conclude from the constant slope that erythritol

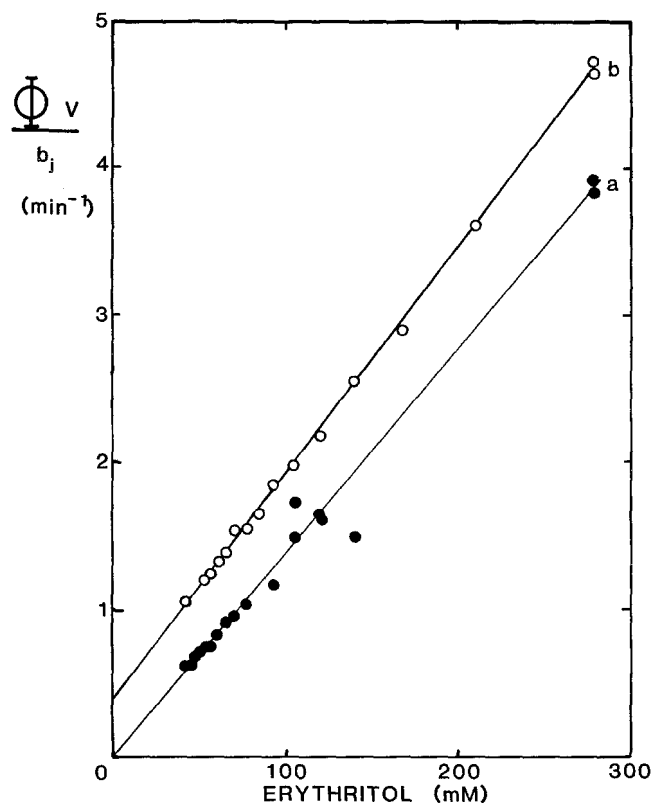


FIG. 7. Initial rates of solute transport as a function of erythritol concentration. The initial rate of swelling, v (min^{-1}), is normalized according to Equation 12 (see text). *Curve a*, normal mitochondria; *Curve b*, preswollen mitochondria.

permeability is independent of matrix volume.

The slopes of the curves in Fig. 7 are 14.6 (*curve a*) and 16.1 (*curve b*) $\text{mM}^{-1} \text{min}^{-1}$. The transport rate constants corresponding to these values can be obtained by multiplying by S_o . Rigorously speaking, S_o is the slope of a gravimetric osmotic curve carried out on each preparation of mitochondria. In practice, it is sufficient to use 190 $\text{nosmol} \cdot \text{mg}^{-1}$ for normal mitochondria, a value which has been found to be reproducible ($\pm 5\%$) (1). Preswollen mitochondria generally contain less solutes, and their osmotic solute content, S'_o , can be estimated by comparing the ratio of the slopes, b'/b_s , of the LS osmotic curves in the reversible region:

$$S'_o = \frac{190b'}{b_s} \quad (13)$$

where b_s is the slope of the reversible part of the LS osmotic curve for normal mitochondria, and b' is the observed osmotic slope for the preswollen preparation. Applying Equation 13 to the data of Fig. 6, *curve b*, we estimate S'_o for this preparation of preswollen mitochondria to be 149 $\text{nosmol} \cdot \text{mg}^{-1}$. Accordingly, the erythritol transport rate constants for normal and preswollen mitochondria, respectively, are found to be 2.77 and 2.40 $\mu\text{l} \cdot (\text{mg} \cdot \text{min})^{-1}$ over a range of osmolalities between 42 and 280 mosm. This corresponds to a range of total matrix water content between 1.0 and 5.0 $\mu\text{l}/\text{mg}$.

Analysis of Swelling Data Using the Integrated Equation—Equation 6 is difficult to apply due to the occurrence of transition points, due to the finite time required to reach osmotic equilibrium (1) and due to the nonlinear relationship between v and t . Use of the integrated equation (Equation 11) should eliminate these difficulties. In order to analyze data

such as those shown in Fig. 4 we must select a range of β values for which the osmotic curve is linear and values of β_0^0 and b_j are known from the osmotic curve. As illustration, Fig. 8 contains traces plotted as $(\beta - \beta_0^0)^2$ versus time. The choice of β_0^0 in the dependent variable dictates that the slopes must be taken in the range between $\beta = 0.29$ and 0.40 (region 3). Inspection of the data in Fig. 8 shows that the traces are linear over this range, as predicted. Similar plots were generated to determine the slopes corresponding to regions 1 ($\beta = 0.12$ – 0.17) and 2 ($\beta = 0.17$ – 0.29) from normal mitochondria and from preswollen mitochondria ($\beta = 0.12$ – 0.40).

According to Equation 11, the slopes of curves such as those in Fig. 8 should be proportional to Φ^{-1} , provided that neither the permeability to erythritol nor the area of the membrane is affected by the osmolality. In accord with this prediction, all four rate curves are linear and intercept the origin (see Fig. 9). According to Equation 11, the slopes of the plots in Fig. 9 are equal to $2c_w b_j^2 k / S_o$. If the permeability to erythritol and membrane area is the same in each segment of the kinetic curve, the large differences in slopes should reflect the different slopes of the osmotic curve. Using the values of b_j from the corresponding osmotic segment and values of S_o from the preceding section, we can calculate k , in $\mu\text{l}(\text{mg}\cdot\text{min})^{-1}$, for each curve in Fig. 9. These values, and the approximate range of matrix volumes to which they pertain, are 2.9 (0.9–1.9 $\mu\text{l}/\text{mg}$), 2.9 (1.9–3.1 $\mu\text{l}/\text{mg}$), and 2.8 (3.1–5.0 $\mu\text{l}/\text{mg}$) for normal

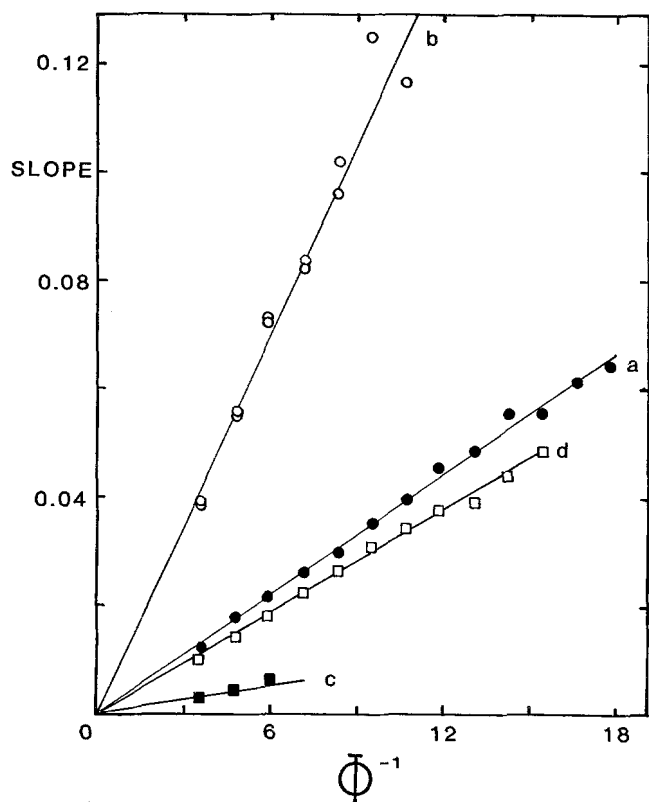


FIG. 9. Analysis of data using the integrated rate equation. Slopes over the appropriate range are obtained from plots, such as those in Fig. 8, of $(\beta - \beta_0^0)^2$ versus time. These slopes are then plotted versus reciprocal osmolality of the medium. As predicted by Equation 11, these plots are linear and intercept the origin. Plot a, slopes taken from the range of $\beta = 0.27$ – 0.45 with $\beta_0^0 = 0.123$. Plot b, slopes taken from the range of $\beta = 0.018$ – 0.27 with $\beta_0^0 = 0.0018$. Plot c, slopes taken from the range of $\beta = 0.14$ – 0.16 with $\beta_0^0 = 0.125$. Plot d, slopes taken from the entire range of $\beta = 0.16$ – 0.45 with $\beta_0^0 = 0.133$, using preswollen mitochondria. Slope of plot a = 0.00369, plot b = 0.012, plot c = 0.00085, plot d = 0.00314.

mitochondria and 3.0 over the entire range (0.9–5.0 $\mu\text{l}/\text{mg}$) for preswollen mitochondria. Thus, the large variation in slopes seen in Fig. 9 is due entirely to the volume-dependent variation in LS response, reflected in the parameter b_j .

Acceleration in Light Scattering Rates Is Independent of Transport Rates—Tedeschi (6) observed acceleration in erythritol but not in malonamide medium, a finding which appears to conflict with a structural interpretation of LS kinetics. Fig. 10 contains typical LS traces of mitochondria swelling in 280 mosm erythritol and malonamide. The erythritol trace is similar to that shown in Fig. 4 except that data points were collected at 10/s. The malonamide trace exhibits faster kinetics, and the acceleration phase is scarcely visible, being complete within 4.5 s of mitochondrial addition. According to our model (1), β is a single-valued function of matrix volume; therefore the kinetic curves for any two solutes should be superimposable when plotted on suitably scaled time axes (see Equation 11). This prediction is evaluated in Fig. 11, in which the time required to reach a specific value of β in erythritol is plotted versus the time to reach the same value in malonamide. The relationship is linear over a range of β which includes the transition at $\beta = 0.17$. Since the ratio of rate constants, k (permeability times area), for the two solutes remains constant as the mitochondria swell, the transitions resulting in changes in b_j must occur at identical values of β for each solute. This observation permits the malonamide trace to be superimposed on the erythritol trace simply by scaling the time values according to the slope of Fig. 11 (open circles, Fig. 10).

Similar experiments were carried out in 110 mosm media, and the results (not shown) were entirely consistent with those contained in Figs. 10 and 11, showing that the ratio of permeabilities remains constant over a 5-fold increase in matrix volume. The ratio of permeabilities was found to be 4.99. This is close to 5.4, the ratio of the half-times of equilibration of malonamide and erythritol in submitochondrial particles (31).

Effects of DCCD and Mg^{2+} Depletion on Ion Pair Transport and on Erythritol Permeability—Fig. 12 contains two traces from mitochondria suspended in 250 mM erythritol. Prior to the assay, one preparation was incubated for 30 min with DCCD (50 nmol/mg), while the other was untreated. Under these conditions, DCCD is found to inhibit Cl^- uniport by

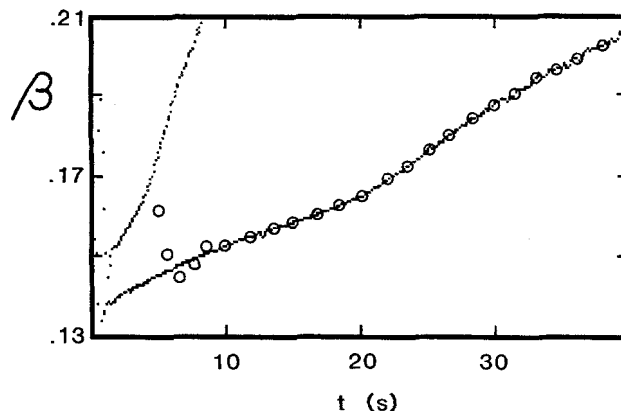


FIG. 10. Comparison of mitochondrial LS kinetics in erythritol and malonamide. Values of β , calculated from A using Equation 1, are plotted versus time after addition of mitochondria (0.1 mg/ml) to the assay medium. The left trace was obtained in 280 mosm malonamide medium and the right trace in the erythritol stock medium (see "Experimental Procedures"). The open circles represent data points from the malonamide trace plotted on a time axis equal to $t/4.99$. This factor was determined from the plot shown in Fig. 11.

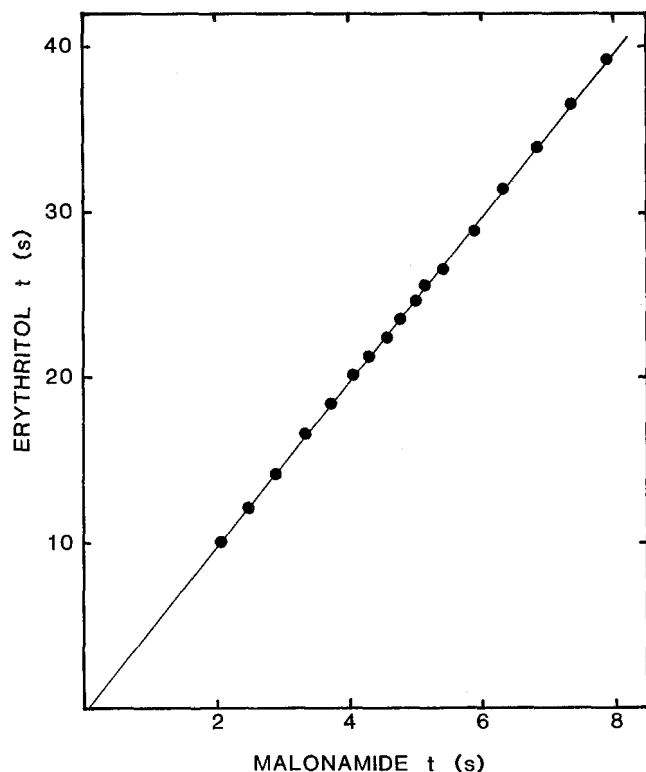


FIG. 11. The ratio of permeabilities to malonamide and erythritol remains constant as mitochondria swell. Using the data from Fig. 10, the time at which the erythritol trace reaches a specific value of β is plotted versus the time at which the malonamide trace reaches the same value. The slope of the curve is 4.99 and represents the ratio of the permeability of the mitochondria to the two solutes.

95% (28), but DCCD clearly has no effect on erythritol transport (Fig. 12). This result has been confirmed in repeat experiments and at different erythritol concentrations. A similar series of experiments has been carried out in NH_4SCN plus quinine with similar results; *i.e.* quinine-induced swelling in NH_4SCN is not affected by DCCD pretreatment.

The same two assays were applied to a comparison of normal and Mg^{2+} -depleted mitochondria. Erythritol permeability was unaffected by Mg^{2+} depletion over a 5-fold range of erythritol concentrations. The values of k were found to be 4.1 ± 0.2 and $4.0 \pm 0.2 \mu\text{l}(\text{mg}\cdot\text{min})^{-1}$ in normal and Mg^{2+} -depleted mitochondria, respectively. The rate of quinine-induced swelling in NH_4SCN is reduced slightly by Mg^{2+} depletion, but the quality of the curves is unaffected. The change in rate can be accounted for by matrix acidification secondary to A23187-induced $\text{Mg}^{2+}/2\text{H}^+$ antiport (32). This results in a reduced gradient for HSCN, the driving force for ion pair mediated transport of SCN^- (30). We conclude that neither DCCD nor Mg^{2+} depletion has any effect on inner membrane permeability to erythritol or to the quinine- SCN^- ion pair.

DISCUSSION

This study demonstrates that the LS technique can be applied to quantitative problems of mitochondrial transport. Considering the complexities, both of the LS response itself and of the transport processes studied, the agreement between data and simple kinetic equations is gratifying. A major reason for this agreement is that the complexities of the relationship between A^{-1} and matrix volume (1) have been taken into account in the analysis of the kinetic data. The procedures presented here are significantly different from previous at-

tempts to quantitate solute transport from changes in LS. Nevertheless, this work represents an advance, not a departure, from the important foundations laid by Tedeschi and Harris (2, 5) and Tedeschi (6, 16).

We also address a particular qualitative question regarding LS kinetics. Do nonlinear kinetics imply a change in transport, or do they reflect a transition in LS properties? This is a question of some moment, since the accelerated rate of swelling observed in Figs. 2 and 4 could be attributed to a real increase in solute flux after matrix volume has reached a certain point. Indeed, the literature is replete with reference to membrane stretching and consequent increase in permeability (18–24). To us, the concept of membrane stretching is at variance with Tedeschi's perceptive concept of inner membrane unfolding (2, 6), supported by the micrographs of Stoner and Sirak (33) and Hunter *et al.* (34). Membrane stretching seems also to be at variance with the very concept of osmotic equilibrium in mitochondria, in which transmembrane pressures do not develop (35). We believe the present results strongly support the alternative explanation, that transitions in the kinetic curves have the same origin as transitions in the osmotic equilibrium curves (1). That is, they arise from irreversible changes in the contribution of membrane packing volume to the total "optical" volume. Thus, the major transition point occurs at the same value of β (0.17) whether matrix volume is changed secondary to changes in water activity (1) or to transport of salts (Figs. 1 and 2) or nonelectrolytes (Figs. 4 and 10), and the transition point disappears from both kinetic and equilibrium curves after preswelling (Fig. 5).

The foregoing merely states that the LS response is the same irrespective of whether mitochondrial swelling is induced by lowered water activity or by solute transport. To determine whether the rate constant increases when matrix volume is expanded, as suggested by Tedeschi (6), we have applied the initial rate equation and the integrated rate equation to erythritol transport in normal and preswollen mitochondria. The data show that osmolality-dependent changes in LS kinetics are paralleled exactly by osmolality-dependent changes in the slope of the osmotic equilibrium curve. Thus, over an 8-fold volume range, we observe no volume-dependent change in the permeability to erythritol when the rates are corrected for the observed osmotic slopes.

While Tedeschi (6) observed acceleration in the LS kinetics in media containing slowly transported solutes, such as mannitol and erythritol, he did not observe acceleration in media containing rapidly transported species, such as malonamide, urea, and glycerol. We believe that he may have missed the "acceleration" phase in rapidly transported solutes because it is so brief (see malonamide curve, Fig. 10). This illustrates an important consideration in the application of LS to transport kinetics: the technique is not well-suited to studies carried out in isotonic media, in which LS is both insensitive and associated with a transition point (1). Transport studies in isotonic media yield kinetic curves whose complexity may be caused by changes in morphological structure rather than changes in permeation rate. For these reasons, it is preferable to study transport in 115 mosm media, at the start of a linear segment of the LS osmotic curve. Nevertheless, any segment of the LS kinetic curve, including that which spans the irreversible transition region, may be used to estimate transport rates, provided the characteristics of the absorbance osmotic curve are known and taken into account.

Comparison of swelling traces in malonamide and erythritol (Figs. 10 and 11) confirms that the acceleration phase in LS kinetics is independent of both the species transported and

the rate of transport. The linearity of the plot in Fig. 11 shows that the relative permeability of the membrane to the two solutes remains constant over a wide range of matrix volumes. These data also show that the LS technique is capable of quantitating very rapid swelling rates secondary to solute transport. The initial rate of transport in 264 mM malonamide approaches 5000 nmol/mg·min.

In seven different mitochondrial preparations, values for the erythritol transport rate constant have ranged from 2.4 to 4.1 $\mu\text{l}(\text{mg}\cdot\text{min})^{-1}$. This is in good agreement with earlier permeability measurements by Tedeschi (6). Using 4.3×10^9 (36) or 7.2×10^9 (37) as the number of mitochondria/mg, his value corresponds to 2.5 or 4.2 $\mu\text{l}(\text{mg}\cdot\text{min})^{-1}$. Mitchell (38) has estimated the inner membrane surface area to be 40 $\text{m}^2\cdot\text{g}^{-1}$. Using a value of 3.0 $\mu\text{l}(\text{mg}\cdot\text{min})^{-1}$ for erythritol transport, we obtain permeability constants for erythritol and malonamide of 1.3×10^{-7} and 6.3×10^{-7} $\text{cm}\cdot\text{s}^{-1}$, respectively. As reported by Thompson and Henn (39), Vreeman obtained a value of 7.5×10^{-7} $\text{cm}\cdot\text{s}^{-1}$ for erythritol permeability in lecithin-decane bilayer membranes.

DCCD has been shown to inhibit several inner membrane ion porters, including the K^+/H^+ antiporter (17) and the anion uniporter (28, 40). Similarly, Mg^{2+} depletion has been shown to activate both of these porters by releasing them from endogenous inhibition by Mg^{2+} (28, 41). The question arises as to how specific these effects are. For example, DCCD interacts with numerous inner membrane proteins (42, 43), and Brierley *et al.* (44) have proposed that Mg^{2+} depletion causes generalized increases in the permeability of the inner membrane. Present results indicate, however, that neither DCCD nor Mg^{2+} depletion interfere with erythritol transport or with quinine-mediated transport of SCN^- across the inner membrane. If these solutes are crossing via nonspecific pathways, it follows that neither DCCD nor Mg^{2+} depletion is inducing generalized permeability changes in the inner membrane of mitochondria.

The LS technique is rapid and simple, and, in many cases, no practical alternative methodology for studying transport is available. This discussion would be incomplete without mention of two advantageous technical features of the system described in Ref. 1. 1) The light probe colorimeter is a simple and inexpensive device which provides reproducible results. To bring the light to the mitochondrial suspension, rather than vice versa, has the advantage of permitting good thermal control and access to the sample. It should be possible to build a chamber containing this and other probes. 2) The analog-digital device and microcomputer-based data acquisition system have proved to be an indispensable aid to this research. For quantitative estimates of transport rates, it is essential to obtain data in a form which is proportional to matrix volume. This parameter is A^{-1} , as shown by Tedeschi and Harris (2, 5) and others (1, 6, 14, 15). Values of A^{-1} can be obtained using a chart recorder, but the signal to noise ratio is rather poor, and reading and converting transmittance values from a chart recording is laborious and cost-ineffective. In contrast, the quality of kinetic recordings using the present device is very high. Converted data can be plotted onto the monitor in real time, regression analyses can be performed, and the data can be stored and a record can be obtained using an inexpensive dot matrix printer.

We conclude that unfolding of the inner membrane, secondary to matrix swelling, has no effect on its permeability to the polar nonelectrolytes, erythritol and malonamide. A more general conclusion from these studies and those of the companion paper (1) is that the LS technique is applicable to

quantitative studies of solute transport across the inner membrane of mitochondria. It is hoped that the present findings will aid in the full exploitation of this powerful technique.

Acknowledgment—We wish to thank Janice Flahiff for expert technical assistance.

REFERENCES

1. Beavis, A. D., Brannan, R. D., and Garlid, K. D. (1985) *J. Biol. Chem.* **260**, 13424–13433
2. Tedeschi, H., and Harris, D. L. (1955) *Arch. Biochem. Biophys.* **58**, 52–67
3. Koch, A. L. (1961) *Biochim. Biophys. Acta* **51**, 429–441
4. Ostler, G. (1955) in *Physical Techniques in Biological Research* (Ostler, G., and Pollister, A. W., eds) Vol. I, pp. 51–71, Academic Press, New York
5. Tedeschi, H., and Harris, D. L. (1958) *Biochim. Biophys. Acta* **28**, 392–402
6. Tedeschi, H. (1959) *J. Biophys. Biochem. Cytol.* **6**, 241–252
7. Klein, R. L., and Neff, R. J. (1960) *Exp. Cell. Res.* **19**, 133–155
8. Honda, S. I., and Muenster, A. M. (1960) *Arch. Biochem. Biophys.* **88**, 118–127
9. Bartley, W., and Enser, M. B. (1964) *Biochem. J.* **93**, 322–330
10. Lehninger, A. L. (1962) *Physiol. Rev.* **42**, 467–517
11. Cleland, K. W. (1952) *Nature* **170**, 497–499
12. Raaflaub, J. (1955) *Helv. Chim. Acta* **38**, 27–37
13. Chappell, J. B., and Perry, S. V. (1954) *Nature* **173**, 1094–1095
14. Massari, S., Frigeri, L., and Azzone, G. F. (1972) *J. Membr. Biol.* **9**, 57–70
15. Massari, S., Frigeri, L., and Azzone, G. F. (1972) *J. Membr. Biol.* **9**, 71–82
16. Tedeschi, H. (1961) *Biochim. Biophys. Acta* **46**, 159–169
17. Martin, W. H., Beavis, A. D., and Garlid, K. D. (1984) *J. Biol. Chem.* **259**, 2062–2065
18. Azzone, G. F., and Piemonte, G. (1969) in *The Energy Level and Metabolic Control in Mitochondria* (Papa, S., Tager, J. M., Quagliariello, E., and Slater, E. C., eds) pp. 115–124, Adriatica Editrice, Bari
19. Azzone, G. F., Massari, S., and Pozzan, T. (1975) *Biochim. Biophys. Acta* **423**, 27–41
20. Azzone, G. F., Bortolotto, F., and Zanotti, A. (1978) *FEBS Lett.* **96**, 135–140
21. Azzone, G. F., Zanotti, A., and Colonna, R. (1978) *FEBS Lett.* **96**, 141–147
22. Bernardi, P., Pozzan, M., and Azzone, G. F. (1982) *J. Bioenerg. Biomembr.* **14**, 387–403
23. Bernardi, P., and Azzone, G. F. (1983) *Biochim. Biophys. Acta* **724**, 212–223
24. Bernardi, P., and Azzone, G. F. (1983) *Eur. J. Biochem.* **134**, 377–383
25. Azzi, A., and Azzone, G. F. (1967) *Biochim. Biophys. Acta* **131**, 468–478
26. Brierley, G. P. (1970) *Biochemistry* **9**, 697–707
27. Selwyn, M. J., Dawson, A. P., and Fulton, D. V. (1979) *Biochem. Soc. Trans.* **7**, 216–219
28. Beavis, A. D., and Garlid, K. D. (1983) *Fed. Proc.* **42**, 1096
29. Jacobs, M. H. (1952) in *Modern Trends in Physiology and Biochemistry* (Barron, E. S. G., ed) pp. 149–171, Academic Press, New York
30. Garlid, K. D., and Nakashima, R. A. (1983) *J. Biol. Chem.* **258**, 7974–7980
31. Berry, E. A., and Hinkle, P. C. (1983) *J. Biol. Chem.* **258**, 1474–1486
32. Reed, P. W., and Lardy, H. A. (1972) *J. Biol. Chem.* **247**, 6970–6977
33. Stoner, C. D., and Sirak, H. D. (1969) *J. Cell Biol.* **43**, 521–538
34. Hunter, G. R., Kamishima, Y., and Brierley, G. P. (1969) *Biochim. Biophys. Acta* **180**, 89–97
35. Garlid, K. D. (1979) in *Cell-Associated Water* (Drost-Hanson, W., and Clegg, J. S., eds) pp. 293–361, Academic Press, New York
36. Gear, A. R. L., and Bednarek, J. M. (1972) *J. Cell Biol.* **54**, 325–345
37. Estabrook, R. W., and Holowinsky, A. (1961) *J. Biophys. Biochem. Cytol.* **9**, 19–28
38. Mitchell, P. (1966) in *Regulation of Metabolic Processes in Mito-*

- chondria* (Tager, J. M., Papa, S., Quagliariello, E., and Slater, E. C., eds) pp. 65-84, Elsevier Publishing Co., Amsterdam
39. Thompson, T. E., and Henn, F. A. (1970) in *Membranes of Mitochondria and Chloroplasts* (Racker, E., ed) pp. 1-52, Van Nostrand Reinhold Co., New York
40. Warhust, I. W., Dawson, A. P., and Selwyn, M. J. (1982) *FEBS Lett.* **149**, 249-252

41. Garlid, K. D. (1980) *J. Biol. Chem.* **255**, 11273-11279
42. Solioz, M. (1984) *Trends Biochem. Sci.* **9**, 309-312
43. Azzi, A., Casey, R. P., and Nałecz, M. J. (1984) *Biochim. Biophys. Acta* **768**, 209-226
44. Brierley, G. P., Jurkowitz, M. S., Farooqui, T., and Jung, D. W. (1984) *J. Biol. Chem.* **259**, 14672-14678

SUPPLEMENT TO

SWELLING AND CONTRACTION OF THE MITOCHONDRIAL MATRIX:

II. QUANTITATIVE APPLICATION OF THE LIGHT SCATTERING TECHNIQUE TO SOLUTE TRANSPORT ACROSS THE INNER MEMBRANE

By Keith D. Garlid and Andrew D. Beavis

EXPERIMENTAL PROCEDURES

The experimental procedures used in this paper have been described in the previous communication (1).

Incubation media - All incubation media were prepared by diluting fresh stock media to obtain the desired solute concentrations. The NH_4SCN stock medium was 275 mosm and contained 146 mM NH_4SCN , 5 mM TES, 0.1 mM EGTA. The pH was adjusted to pH 6.8 to minimize activation of the pH-dependent anion conducting pore (25-28). The erythritol stock medium was 280 mosm and contained 264 mM erythritol, 5 mM TES and 0.5 mM EGTA. The malonamide stock medium was identical except for the replacement of erythritol with malonamide. The pH was adjusted to pH 7.1 with KOH. Rotenone was added to each incubation at a concentration of 2 $\mu\text{g}/\text{mg}$ mitochondrial protein.

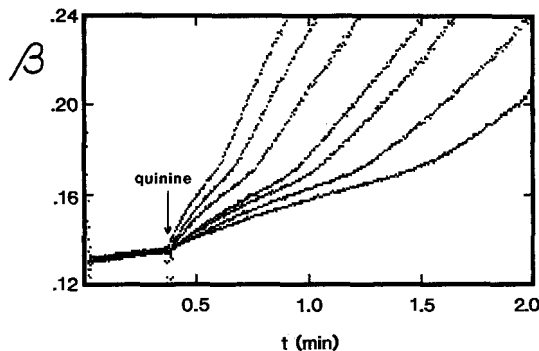


Fig. 1. Effect of quinine concentration on mitochondrial L.S. kinetics in NH_4SCN . Values of β , calculated from A using Eq. (1), are plotted versus time after addition of a small volume of mitochondria to the NH_4SCN stock assay medium (275 mosm) containing nigericin (1 nmol/mg). Nigericin was included in the medium to equilibrate K^+/H^+ antiport (30). Swelling was initiated by addition of quinine at 0.36 min. Rates of swelling increase with increasing concentration of quinine. Proceeding from the rightmost curve, quinine concentrations were 40, 60, 80, 100, 150, 200 and 250 μM .

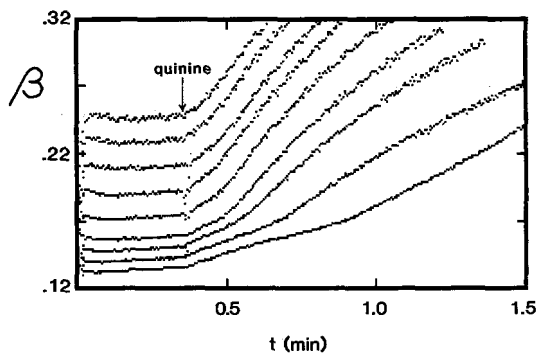


Fig. 2. Effect of osmolality on L.S. kinetics of quinine-induced swelling in NH_4SCN . The experiment was carried out as described in the legend to Fig. 1 except that a constant dose of 100 μM quinine was added at 0.36 min and the NH_4SCN stock medium was diluted to give the following osmolalities: 55, 61, 69, 79, 92, 110, 138, 183, 275 mosm. The starting level of each curve increases with decreasing osmolality.

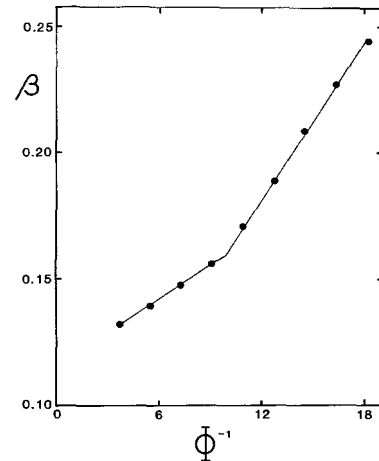


Fig. 3. Absorbance osmotic curve obtained in NH_4SCN . These data are derived from the traces presented in Fig. 2. The values of β were determined from each trace at 0.1 min prior to the addition of quinine and are plotted versus reciprocal osmolality, Φ^{-1} .

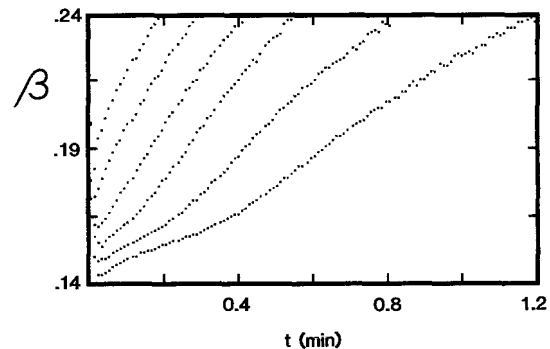


Fig. 4. Effect of osmolality on the mitochondrial L.S. kinetics in erythritol. Values of β , calculated from A using Eq. (1), are plotted versus time after addition of mitochondria (0.1 mg/ml) to the assay medium. The assay media were prepared by diluting the erythritol stock medium described under "Experimental Procedures". Initial values of β increase with decreasing osmolality. Osmolalities used were 105, 120, 140, 180, 210 and 280 mosm.

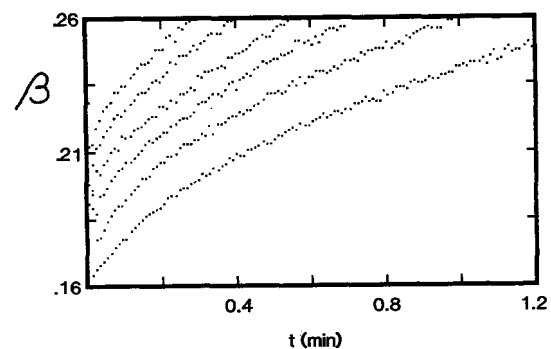


Fig. 5. Effect of mitochondrial preswelling on L.S. kinetics in erythritol media. This experiment was carried out exactly as described in Fig. 4 and at the same osmolalities; however in this case the stock of mitochondria had been hypotonically preswollen and reisolated in 0.25 M sucrose as described previously (1).

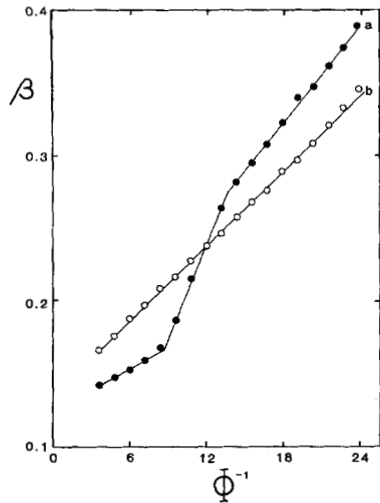


Fig. 6. Absorbance osmotic curves obtained in erythritol media. Initial values of β_0 , calculated by extrapolating kinetic plots to zero time, are plotted versus the reciprocal osmolality of the medium, Φ^{-1} . These data were obtained from the experiments shown in Figs. 4 and 5, extended to include measurements in media of osmolalities down to 42 mosm. Curve a, normal mitochondria; curve b, preswollen mitochondria. Slopes (b_j , osmolal) and intercepts (β^0_j) for the different segments: Curve a; $b_1 = 0.005$, $\beta^0_1 = 0.125$; $b_2 = 0.0198$, $\beta^0_2 = 0.0018$; $b_3 = 0.0112$, $\beta^0_3 = 0.123$; Curve b, $b = 0.0088$, $\beta^0 = 0.133$.

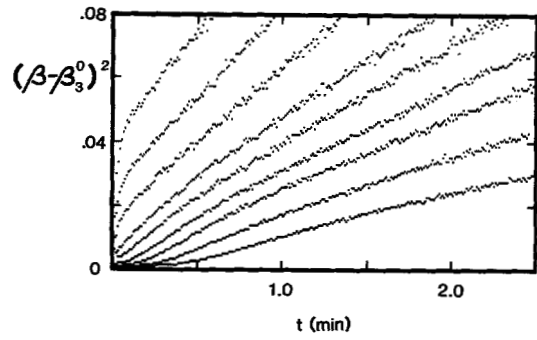


Fig. 8. Plot of $(\beta - \beta_3^0)^2$ versus time for mitochondria swelling in erythritol at different osmolalities. These curves were calculated from the traces of the experiment of Fig. 4. The value of β_3^0 is 0.123, obtained from analysis of Fig. 6. The slopes of these curves measured in the range of $(\beta - \beta_3^0)^2 = 0.02$ to 0.08 are plotted as curve a in Fig. 9.

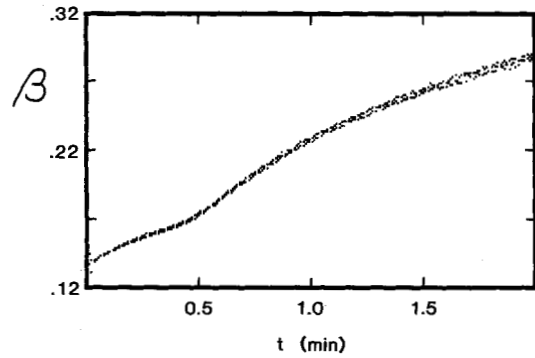


Fig. 12. DCCD has no effect on erythritol transport. Values of β ($\text{mg}\cdot\text{ml}^{-1}$), calculated from A using Eq. (1) are plotted versus time after addition of mitochondria (0.1 mg/ml) to the 280 mosm erythritol assay medium described in "Experimental Procedures". One curve in the figure was obtained from an untreated stock suspension and the other from a suspension incubated with DCCD (50 nmol/mg) for 30 min at 0°C.